Available online at www.sciencedirect.com
ScienceDirect
Computer-Aided Design 40 (2008) 235–243
COMPUTER-AIDED DESIGN
www.elsevier.com/locate/cad

Extruder path generation for Curved Layer Fused Deposition Modeling

Debapriya Chakraborty, B. Aneesh Reddy, A. Roy Choudhury*

Department of Mechanical Engineering, Indian Institute of Technology, Kharagpur-721302, India

Received 13 March 2007; accepted 28 October 2007

Abstract

Extruder path generation for a new rapid prototyping technique named "Curved Layer Fused Deposition Modeling" (CLFDM) has been presented. The prototyping technique employs deposition of material in curved layers in contrast to flat layers as in Fused Deposition Modeling (FDM). The proposed method would be particularly advantageous over FDM in the manufacturing of thin, curved parts (shells) by reduction of stair-step effect, increase in strength and reduction in the number of layers. The criteria for the generation of tool paths for CLFDM are proper orientation of filaments and appropriate bonding between adjacent filaments in same layer and in successive layers.

Keywords: Fused Deposition Modeling; Rapid prototyping; Skull bone; Layered manufacturing

1. Introduction

Rapid prototyping (RP) refers to a group of solid freeform fabrication (SFF) processes that are capable of developing complex shapes without part-specific tooling in a short span of time. Newer RP processes are being developed and commercialized every year [1]. Layered Manufacturing (LM) technology is employed for most of the RP processes wherein a part is produced by employing layer-by-layer deposition of material. Fused Deposition Modeling (FDM) is one of the commercially exploited LM processes where a filament of heated (fused/semi-solid) thermoplastic material is extruded through a deposition nozzle (which would henceforth be referred to as the 'extruder' in this article) and applied over a flat surface to form a layer (Fig. 1). The main advantage of LM over conventional manufacturing is that complex shapes can be physically realized without elaborate tooling. However, there are some specific part shapes like thin, slightly curved shell-type structures (skull bones, turbine blades etc.) where the application of LM is poorly suited and may result in lack of strength, stair-step effect (poor surface finish) or large number of layers (higher build time) [2]. The reason behind such low part quality is the discontinuous nature of the filaments in building up the part by LM (Fig. 2).

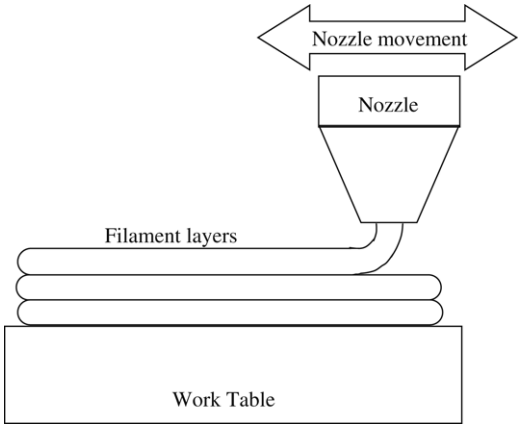

Fig. 1. Schematic diagram of FDM.

Strength of parts made by FDM suffers from anisotropy [3] and adhesive strength between layers (or across filaments) is appreciably less than the strength of continuous filaments (longitudinal strength). Zhong et al. [4] studied the mechanical properties of short fiber-reinforced ABS polymers for use as a FDM feedstock material. On comparison of the longitudinal strength with the adhesive strength, it was observed that the former was substantially higher than the latter. Hence, discontinuity of filaments on the part shown in Fig. 2 produced by FDM would tend to reduce its strength. Apart from this, there is pronounced stair-step effect in the sample of Fig. 2 and it is obvious that layer thickness would have to be appreciably

* Corresponding author. Tel.: +91 3222 282970, +91 9434036694 (mobile); fax: +91 3222 255303.
E-mail addresses: debapriya.chakraborty@iitkgp.ac.in (D. Chakraborty), archie@mech.iitkgp.ac.in, archie@mech.iitkgp.ernet.in (A. Roy Choudhury).

0010-4485/$ - see front matter © 2007 Elsevier Ltd. All rights reserved.
doi:10.1016/j.cad.2007.10.014

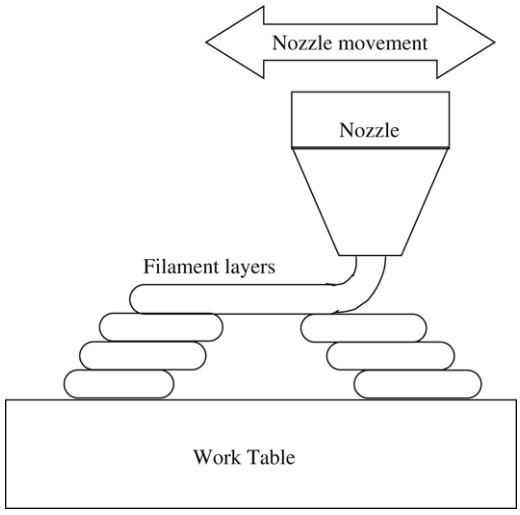

Fig. 2. Prototyping of a thin curved part in FDM.

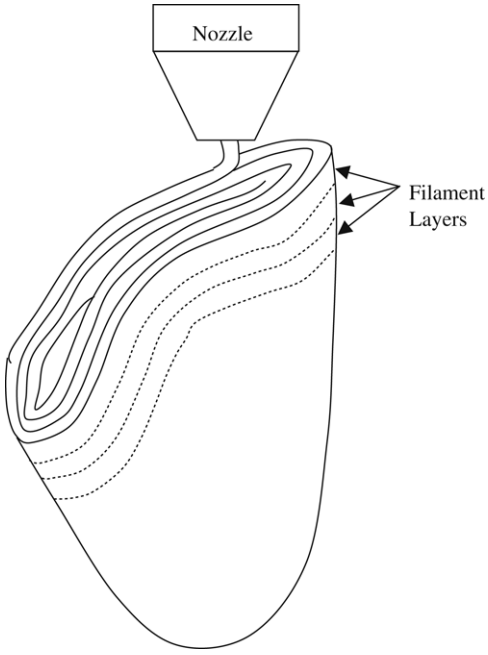

Fig. 3. Choice of build direction to achieve continuous filaments in thin sections.

reduced in order to achieve better surface finish. This in turn would increase the build time, as mentioned earlier.

However, in a number of cases, proper choice of orientation of the part (build direction [5–8]) in the FDM chamber may eliminate some of the above-mentioned drawbacks. For example, in the case of a typical curved thin part under consideration, continuity of filaments can be obtained in the concerned section of the part if it is held upright (Fig. 3) in the deposition chamber and the deposition carried out as shown (contour fill). However, discontinuity of filaments would still exist across these sections shown by dotted lines. In fact, there would not be any continuous fibers across these sections. Further, if the part has bi-directional curvature (Fig. 4) the selected build orientation would not serve the purpose.

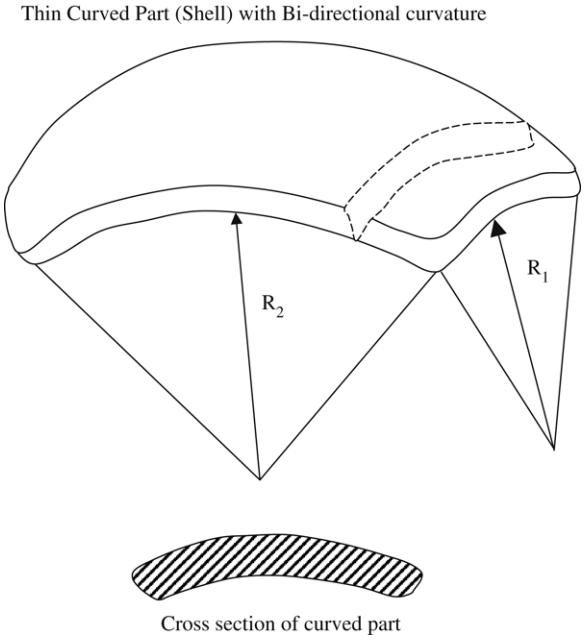

Fig. 4. Typical example of a thin curved part with bi-directional curvature.

Adaptive slicing is perhaps the main strategic response of FDM to solve these problems. Thinner layers in regions of low (near-horizontal) surface slope and high curvature would certainly reduce the surface roughness. At the same time, build time is not expected to increase substantially as higher layer thickness would be retained in places of high (vertical or near-vertical) surface slope and low curvature. However, the improvement in strength of the part due to thinner layers would be marginal. Further, if thinner layers are applied only at selected regions (the very idea of adaptive slicing), the part would remain as weak as the thick-layered regions. In the available literature, one may find a number of attempts for adaptive slicing of parts [9–15], which include both direct slicing and slicing of faceted surfaces in the form of STL files.

"Curved layer FDM" or CLFDM — as proposed in this work, may offer solutions to most of these issues for thin curved shell-type parts as discussed above. In this process, which proposes an entirely new building paradigm for FDM, the filaments would be deposited along curved (essentially non-horizontal) paths instead of planar (horizontal) paths.

If the literature is considered on RPT (Rapid Prototyping Technology) in general, the idea of curvilinear (non-horizontal) material deposition is not entirely new in other spheres of additive manufacturing. Klosterman et al. [16] have developed curved layer LOM (Laminated Object Manufacturing) process for monolithic ceramics and ceramic matrix composites (CMC). The advantages of this curved layer process are elimination of stair-step effect and improved surface quality, increased build speed, reduced waste, and easier decubing. Researchers from CREDO Laboratory, Clemson University [17] had started an endeavor on variable slice orientation in SLA process. Significant improvement in surface quality due to deposition at variable slice orientation had been envisaged. Kerschbaumer et al. [18] presented an algorithm for generating tool path for 5-axis laser cladding using adaptive slicing

technology. It approximates the tessellated CAD model with a parametric surface and generates the tool paths by varying one of its parameters (Isoparametric paths). Although the generation of tool path is straightforward, isoparametric paths suffer from a major drawback of obtaining denser tool paths in some surface regions than others due to non-uniform transformation between the parametric and the Euclidean spaces [19].

The objective of the present work is the investigation for the manufacturing of curved thin parts by depositing material in curved non-horizontal layers using FDM. It is envisaged that there would be substantial improvement in the mechanical properties of thin-section curved shell-type parts made by CLFDM in comparison to FDM. It is also aimed to develop and implement an algorithm for generating 3D curved paths of the extruder head for filament deposition to achieve successful reproduction of part shape and proper inter-filament bonding.

With the development of bio-friendly materials, RP has been exploited in the field of biomedical engineering [20], which requires precision and flexibility. Biocompatible PMMA-resin was used for developing the part of a skull for replacement in the case of an accident victim [21]. The proposed method of CLFDM would be very appropriate for the manufacturing of functional prototypes of skull bones and other thin shell-type parts. Other potential applications are in the manufacturing of intricate and small sized turbine blades or objects of thin cross-section, produced for actual use or for design, verification and testing. The advantages of using CLFDM are — lesser number of layers for identical part, higher continuity of filament resulting in more strength and more bonding between consecutive layers (due to larger area of inter-layer bonding).

2. Process description for CLFDM

In FDM, 3-axis CNC is sufficient for the deposition of filaments in a flat layer. In CLFDM, the ideal choice would be a 5-axis CNC machine, such that the extruder axis would always coincide with the normal to the layer at the point of deposition. However, a 3-axis machine would also suffice when this surface normal (**n**) does not appreciably deviate from the vertical (Fig. 5). This condition is valid for slightly curved parts.

FDM uses 2C, P (x- and y-axes with contouring control and z-axis with Point-to-point control) control for the table and head movement. CLFDM has to necessarily use 2C, L (x- and y-axes with contouring control, z-axis with linear interpolation control) control because the table should have a 3D linear interpolator for the deposition of curved layers instead of point-to-point control. Contouring control is retained along x- and y-axes to permit flat-layered FDM with contour-fill if required.

The deposition of the filaments should be done in alternate directions for successive curved layers (Fig. 6). This would reduce voids between layers, strengthen bonds between filaments and increase isotropy by alternate orientation of continuous filaments in the part.

2.1. Determination of filament orientations and interval

First of all, the filament paths (FP) have to be determined for proper reproduction of the part shape by CLFDM. Further,

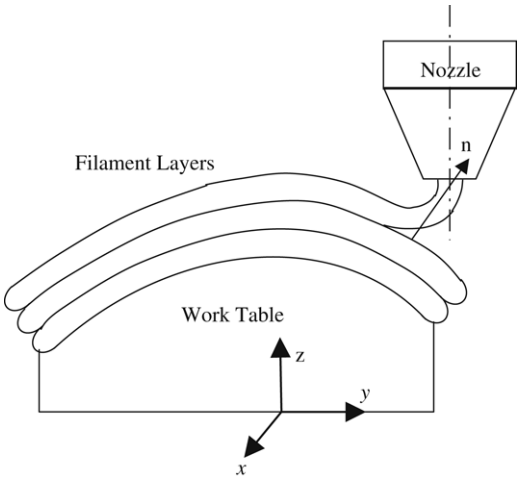

Fig. 5. Prototyping of parts by CLFDM using 3-axis control (x, y and z).

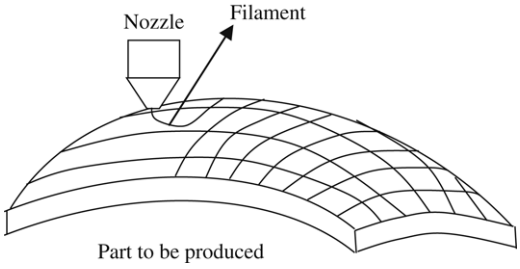

Fig. 6. Prototyping of thin curved part in CLFDM — deposition of filaments in alternate directions for isotropy.

in the case of CLFDM, adjacent filaments (roads) do not necessarily lie on the same plane. Hence, proper lateral bonding between the filaments is an important aspect in this process. In the case of conventional FDM, the filaments in a layer are all in a single plane; hence the maintenance of a constant extruder path interval ensures that the adjacent filaments (roads) would have uniform lateral overlap/superposition (negative gap) and hence uniform lateral bonding along their respective lengths.

In the present work, the filament location (position of the cross-section of the filament at a point on the free form surface) would be planned so as to have a constant superposition with the lower surface (would henceforth be referred to as "previous surface") as well as with the adjacent filament(s). This would ensure uniform bonding between adjacent filaments and between adjacent layers. It is assumed here that the filaments of material extruded in CLFDM are of circular cross-section with a constant diameter throughout the process. The adjacent filament cross-sections are constrained by a pre-specified superposition (realized through a constant common chord of contact (CC)) between the superposed adjacent filament (circular sections) and also inter-layer (curved) overlap throughout the path to achieve uniform lateral bonding.

Initially, the mandrel would be formed by the procedure discussed in Section 2 and thereafter, layers of material extruded by FDM would be laid on it to build up the part. Top surface of the mandrel corresponds to the lower surface of the thin curved part to be prototyped. The strategy here would be to

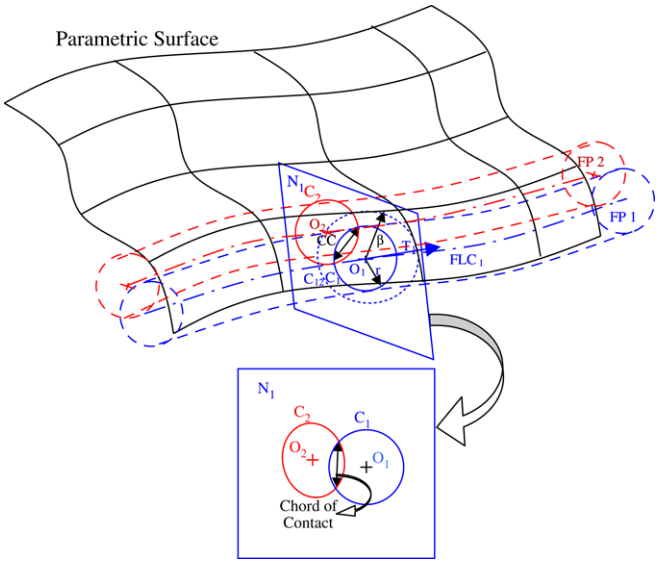

Fig. 7. Procedure for the determination of adjacent filament paths or roads.

build curved layers from the bottom towards the top till the part is fully reproduced (bottom up).

Filament cross-section locations are determined by two sequential steps — initial guess point determination and correction of each point to satisfy the desired strength requirement (constant common chord). A given FP is used to identify the next FP. The initial FP (FP_1) is chosen arbitrarily, preferably, along or very close to one of the edges of the bottom surface of the part. Points along this isoparametric edge of the surface are first selected to be contact points between filament and previous surface/mandrel as the case may be.

The center of the circular cross-section of a filament (to be referred to as Filament location point or FLP) would lie on a surface (OS) offset from previous surface by α (along outward normal to previous surface at every point) given by:

$$\alpha = r - s \tag{1}$$

where r = filament radius and s = pre-set superposition between layers.

This offset surface would be referred to as OS while explaining the details of Fig. 7.

Procedure for the determination of FP_2 *and* FLP_2: A set of FLP points in sequential order obtained along FP_1 is splined to obtain continuous and smooth filament location curve FLC_1 (Fig. 7). The circular cross-sections of the filament at specific FLP are oriented normal to the tangents of FLC_1.

Step 1: With center O_1 and radius r, a circle C_1 is drawn which represents the circular cross-section of FP_1 at O_1. Now, with center O_1 and radius $\beta = \sqrt{(4r^2 - c^2)}$, where c is the desired chord of contact, a circle C_{12} is drawn in N_1 to cut the trace of OS on N_1 at O_2 (as shown in Fig. 7). T_1 and N_1 are respectively the associated tangent and normal plane to FLC_1 at point O_1. If a circle C_2 is drawn with center O_2 and radius r on N_1, it would have the requisite superposition with C_1. However, this procedure constrains the adjacent filament cross-section C_2 to be coplanar with C_1. For this reason — it is not a correct solution and would result in path errors if followed. However, it could be well adopted as a good guess point for searching for a correct adjacent filament cross-section location.

Step 2: Hence, as a correction methodology, all FLP on the next FP (FP_2) are obtained with coplanar approximation and a smooth curve (FLC_2) is passed through them. The circular cross-section of FLC_2 with center at O_2 actually lies on a plane N_2 which is normal to FLC_2 at O_2 (Fig. 8). Now, the intersection of FLC_1 with N_2 yields O_1'. If $O_2O_1' = \sqrt{(4r^2 - c^2)}$, O_2 is accepted as a correct FLP_2. Otherwise, several iterations of the procedure are carried out with radius of circle $C_{12} = \sqrt{(4r^2 - c^2)} \pm \Delta r$ accordingly as $O_2O_1' \langle \text{or} \rangle \sqrt{(4r^2 - c^2)}$ where Δr is a small fraction of $\sqrt{(4r^2 - c^2)}$.

2.2. Formulation

For a parametric surface represented by $\mathbf{P}(u, v)$, an offset surface could be obtained using:

$$\mathbf{P}_{\text{off}} = \mathbf{P}(u, v) + \mathbf{n}\boldsymbol{\alpha} \tag{2}$$

where $\mathbf{n}$ is the unit normal vector for the surface $\mathbf{P}$ can be calculated from:

$$\mathbf{n} = \frac{\mathbf{P}_u \times \mathbf{P}_v}{|\mathbf{P}_u \times \boldsymbol{P}_v|} \tag{3}$$

where $\mathbf{P}_u$ and $\mathbf{P}_v$ represents the partial derivatives of $\mathbf{P}$ with respect to u and v respectively. The value of α is defined with respect to Eq. (1). The parametric equation of the surface formed by the envelope of filament paths is derived by forming a general curve (FLC) in a movable work coordinate system along FP as shown in Fig. 8. The local Cartesian system $x_w y_w z_w$ is created by setting a point on the FLC as the origin (O_1), the surface normal $\mathbf{n}$ (given by Eq. (3)) as the z_w-axis, the tangent to the FLC as the y_w-axis and the third perpendicular direction to be x_w-axis. $\mathbf{i}_w$, $\mathbf{j}_w$, $\mathbf{k}_w$ are the unit vectors in the positive x_w, y_w and z_w directions which are given at any point as:

$$\mathbf{k}_w = \boldsymbol{n} \tag{4a}$$

$$\mathbf{j}_w = \frac{\mathbf{FLC}'(t)}{|\mathbf{FLC}'(t)|} \tag{4b}$$

$$\mathbf{i}_w = \mathbf{j}_w \times \mathbf{k}_w \tag{4c}$$

where $\mathbf{FLC}'(\mathbf{t})$ represents the derivative of the splined path of the filament location curve (FLC).

The generating curve of the filament path envelope surface is a circle of radius r (filament radius) and it can be described in (r, θ) coordinate in the (x_w, z_w) plane as:

$$A_w(\theta) = \begin{bmatrix} r\cos\theta \\ 0 \\ r\sin\theta \end{bmatrix}. \tag{5}$$

Eq. (5) is transformed to the fixed coordinate system XYZ using a rotation and a translation to obtain:

$$\mathbf{A}_m(t, \theta) = {}^{M}_{w}[A]\,\mathbf{A}_w(\theta) + \mathbf{FLP}_1 \tag{6a}$$

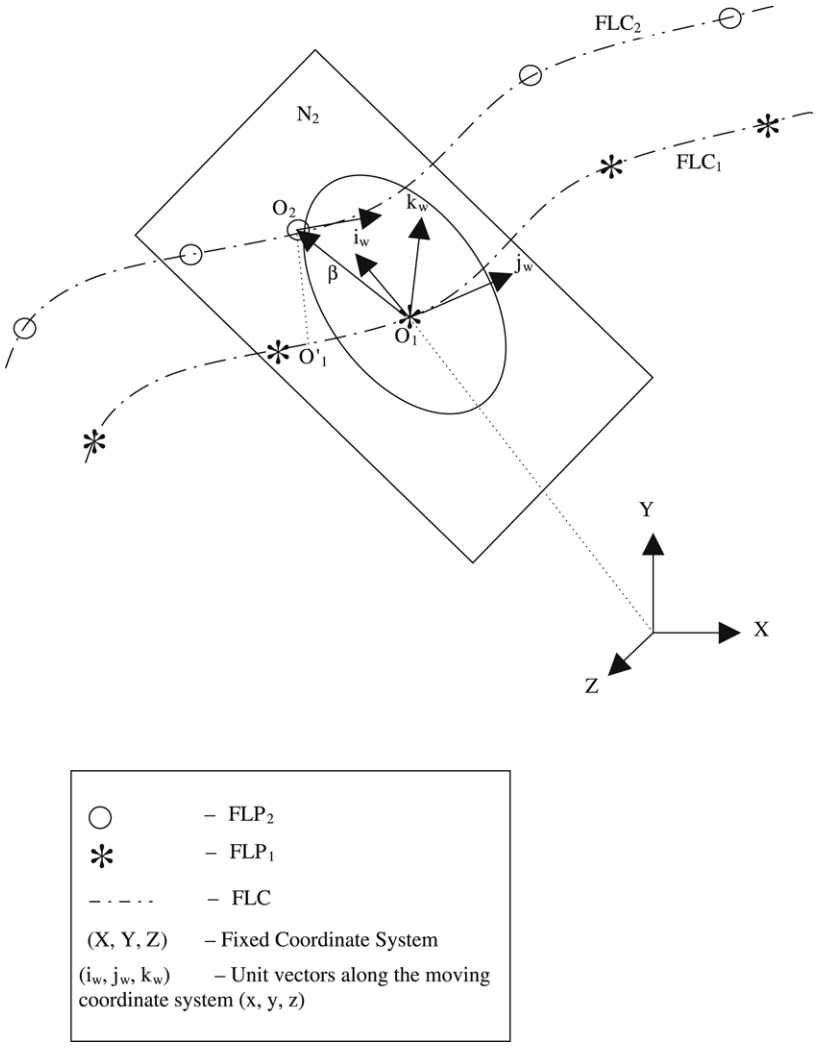

Fig. 8. Identification of coordinate systems and determination of corrected FLC.

$$ {}^{M}_{w}[A] = \begin{bmatrix} \mathbf{i}_w & \mathbf{j}_w & \mathbf{k}_w \end{bmatrix} \tag{6b} $$

$$ \mathbf{FLP}_1 = \begin{bmatrix} X_{\mathrm{FLP}}(t) \\ Y_{\mathrm{FLP}}(t) \\ Z_{\mathrm{FLP}}(t) \end{bmatrix} \tag{6c} $$

where ${}^{M}_{w}[A]$ is the matrix for transforming (x_w, y_w, z_w) to (X, Y, Z).

The initial set of points on FP_2 is obtained with Eqs. (2) and (6a) by solving the equation:

$$ \mathbf{P}_{\mathrm{off}} - \mathbf{A}_m = 0. \tag{7} $$

It is difficult to solve directly Eq. (7) and hence, the problem is modified by adopting a numerical scheme to find the closest point on the design surface which minimizes the function [22]:

$$ \mathbf{F}(u, v) = \mathbf{P}_{\mathrm{off}}(u, v) - \mathbf{A} \tag{8} $$

where $\mathbf{A}$ is a point on the circle. Newton's method is employed to solve Eq. (8) using iterative scheme:

$$ \begin{bmatrix} u^k \\ v^k \\ \theta^k \end{bmatrix} = \begin{bmatrix} u^{k-1} \\ v^{k-1} \\ \theta^{k-1} \end{bmatrix} - (\mathbf{J})^{-1} \times \mathbf{F} \tag{9} $$

where $\mathbf{J} = \begin{bmatrix} \frac{\partial F_x}{\partial u} & \frac{\partial F_x}{\partial v} & \frac{\partial F_x}{\partial \theta} \\ \frac{\partial F_y}{\partial u} & \frac{\partial F_y}{\partial v} & \frac{\partial F_y}{\partial \theta} \\ \frac{\partial F_z}{\partial u} & \frac{\partial F_z}{\partial v} & \frac{\partial F_z}{\partial \theta} \end{bmatrix}$ represents the Jacobian matrix described by the partial derivatives of the function $\mathbf{F}$, with F_x, F_y and F_z are the X, Y and Z components respectively in fixed coordinate system.

3. Results and discussion

The skull shown in the Fig. 9(a) as obtained from [2] is produced by SLA (Stereolithography) which is a LM process. It is included as an example to show an extreme case of stair-step effect — especially at the top dome region. Fig. 9(b) shows the same part (the top dome, a typical thin curved part) if it be made by CLFDM. This graphical simulation of the part Fig. 9(b) is obtained by using the approach outlined for the extruder trajectory in CLFDM. Only two deposition layers are shown for the clarity of the figure. The overlap of the adjacent filaments as well as the inter-layer overlap can be observed in the figure. The comparison evidences the reduction of the stair-step effect in the case of CLFDM compared to that in a LM process. Fig. 9(c)

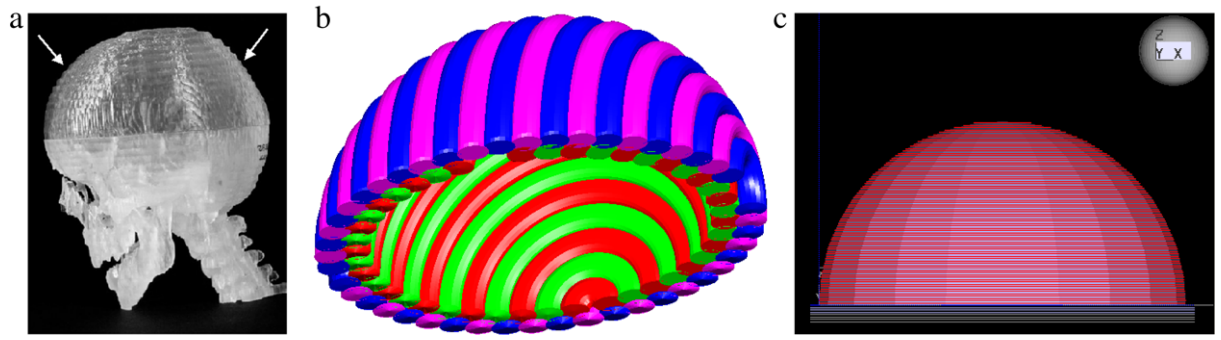

Fig. 9. (a) Model of a skull prototyped using Layered Manufacturing Process (stereolithography), reproduced from [2]. (b) Simulated model of the skull developed with deposited filaments in CLFDM. Two layers are shown with alternate layers of filament discerned by colors. (c) Skull dome made by FDM process with 0.33 mm thick layers.

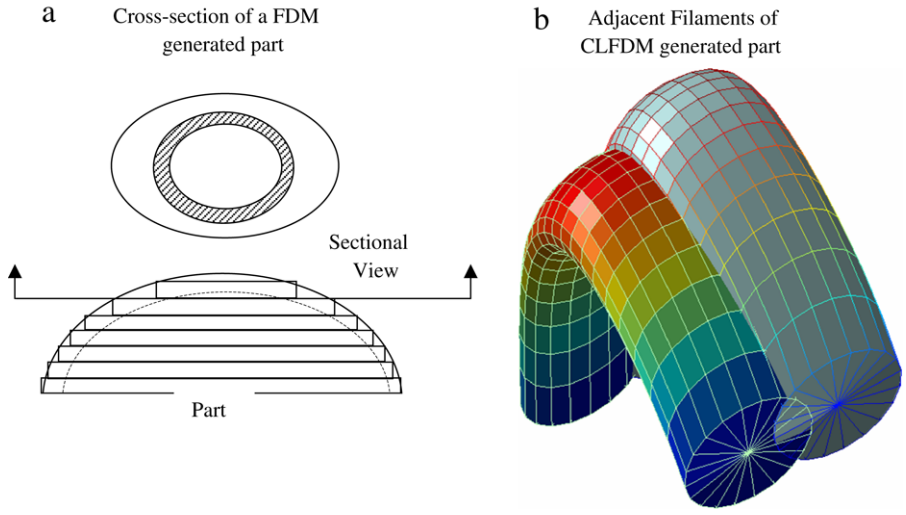

Fig. 10. (a) Sectional view of a part produced by FDM. The overlapped section of two adjacent layers in FDM is shown by shaded lines. (b) Adjacent filaments of CLFDM.

shows the layers if the skull dome be made by FDM process with considerably lower value of layer thickness (0.33 mm). In such a case, stair-step effect is not very pronounced except at the very top, but the number of layers is extremely high (=71). In comparison, if the skull dome thickness is 5.42 mm, around 20 curved layers would be required to build the part using CLFDM. The overlap of the adjacent layers, deposited alternately, was also taken under consideration in obtaining the desired thickness of the part.

As already discussed, the longitudinal tensile strength of the filaments is higher than the bonding strength between adjacent filaments resulting in anisotropy [3,23,24]. In many cross-sections of the FDM-generated part, there is no continuity of filaments (e.g., in the flat inter-layers). A tensile force across, or a shear along the flat inter-layer of a FDM-generated part would be resisted primarily by the inter-filament bonds between layers. In the case of the same part made by CLFDM, the inter-layers are not flat and they tend to span the whole extent of the part. Hence, the inter-layer area per layer is considerably higher if CLFDM is the process instead of FDM. This makes the inter-layers of the CLFDM-generated part considerably stronger than those of the FDM-generated part. Fig. 10 shows the comparison between the contact areas between the layers of the two methods. In Fig. 10(a), it can be seen that one layer is in contact with the layer above it through a thin annular area, while the filaments are deposited in CLFDM ensuring sufficient overlap with a suitable chosen chord of contact between the tubes. As a result, the shear strength of the parts created from conventional FDM would be very low towards the top while in CLFDM a strong bonding is ensured. Moreover, CLFDM creates a woven net-like structure (Fig. 6) which would provide the part more uniform in strength. It is true that cross raster-fill in the case of FDM would provide similar improvements in FDM-generated parts, but it would not increase inter-layer adhesion strength. For these reasons, it can be argued, that CLFDM-generated parts would possess higher strength than identical parts made by FDM.

Commonly, computer tomography (CT) scan produces the axial images that form the basis of 3D CT scans. However, in some cases the scaffold may be inclined at an angle commonly known as gantry tilt. When a set of 2D slices is combined into an image volume for 3D modeling, the gantry angle must be

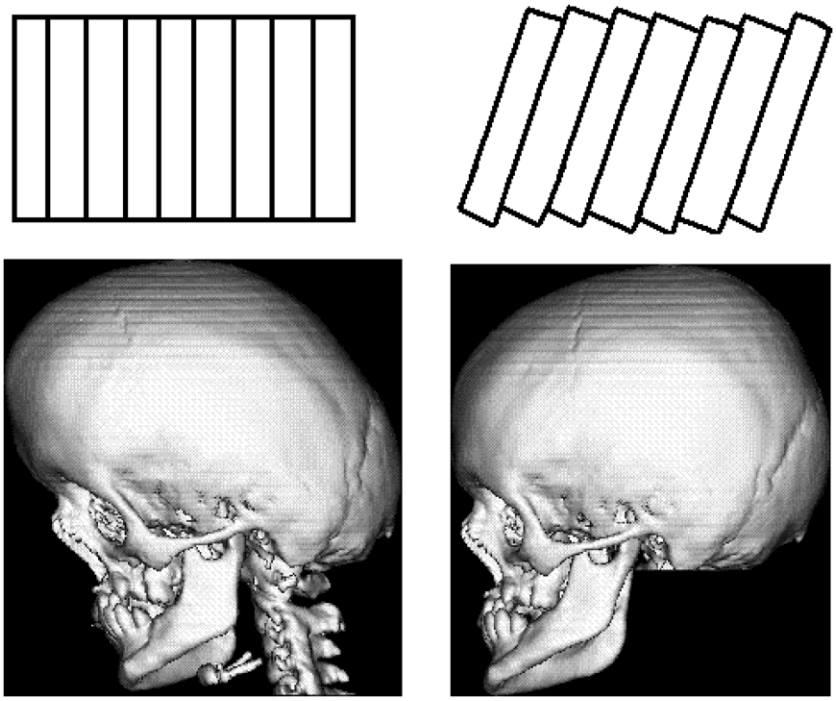

Fig. 11. Geometric distortion effect of gantry tilt on a 3D surface rendered skull (*left*) and the same data after correction (*right*).

taken into account. Fig. 11 obtained from [2] shows the effect with and without gantry tilt. FDM can be implemented after the paths have been transformed using the affine transformations. The build direction does not pose a problem in CLFDM. The 5-axis control can be easily utilized to take care of gantry tilts and hence can fabricate such model easily.

Most engineering surfaces are complex in nature and cannot be described by a simple free form surface patch. There can be surfaces made of multi-patches such that there are abrupt changes in slope and curvature at intersection curves. Some surfaces have patches with circular or non-circular apertures and trims. The parametric image of such trimming 3D space curves (boundaries of the portions to be trimmed) are calculated on the offset surface *OS* for the removal of the portions to be trimmed [25,26]. The CLFDM roads are obtained as described earlier in Sections 2.1 and 2.2. In the case of surface with the trimmed surfaces at the ends, the FLP do not alter and remain same as the older FLPs with an additional truncation of the ends as shown in Fig. 12(a). If trimming of the part appears inside, the FLPs can be constructed in two different approaches as shown in Fig. 12(b) and (c). In Fig. 12(b), the filaments are deposited in a discontinuous manner. The flow of the extruder is stopped at the trimmed region. However, such a discontinuity of filaments may reduce the strength of the part. An alternative approach has been shown in Fig. 12(c) where the continuity of the filaments is preserved. In Fig. 12(d), a third kind of surface is considered where the surface is generated using two different patches. It can be observed in the figure, that the surface patches are not treated in isolation and continuous filament paths are constructed so as to obtain higher strength through continuous filaments or roads.

Turbine blades are thin parts having curvatures in different direction for operating requirements. A typical blade surface is described by a parametric surface and the upper surface is considered for the generation of the FLCs as shown in Fig. 13 (Only one layer of FLCs are shown for clarity.). It can be seen that the FLCs produced are continuous which would provide higher strength compared to discontinuous filaments if made through the existing LM processes.

In 3-axis and 5-axis machining, the basic criterion for tool path generation (determination of tool path intervals) is to obtain acceptable surface roughness. The roughness is produced by scallops left as uncut material between tool paths. The ultimate aim is to produce uniform scallops and this criterion gives rise to isoscallop [22] cutter paths. However, in 5-axis machining, cutters also need to be oriented in a manner so as to avoid gouging with surface being machined. This could also pose similar problem in the case of CLFDM where the periphery of the deposition head could interfere with the part being built up. Hence, in the case of CLFDM, deposition head shape would have to be modified (preferably convex shape with extruder aperture at the tip) to avoid such phenomenon.

It should be noted, that generated paths obtained by the method of offsetting [27,28] may lead to the development of cusps and self-intersections. When the offset distance is larger than the minimum radius of curvature of the object/surface (at the point of deposition and in the direction of the road), a self-intersection in the road is likely to occur. This is possible in intersecting surface patches (Fig. 12(d)). In such cases, self-intersections and loops need to be detected and removed [29]. The offset of parametric surface is finally obtained by applying continuity conditions and smoothening [30].

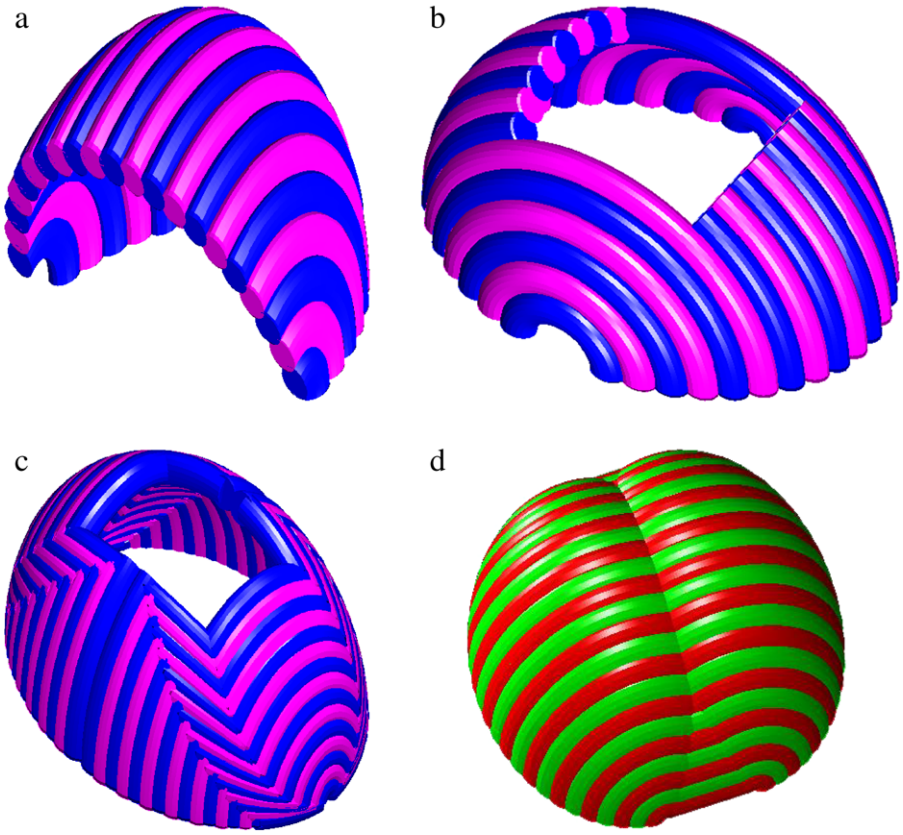

Fig. 12. Model development of different complex geometries using CLFDM — (a) A hemispherical surface with a straight trim on one side (b) Trimmed surface of a part in the interior, discontinuous filament deposition method (c) Trimmed surface of a part in the interior, continuous filament deposition method (d) Surface made of two patches, continuous filament method.

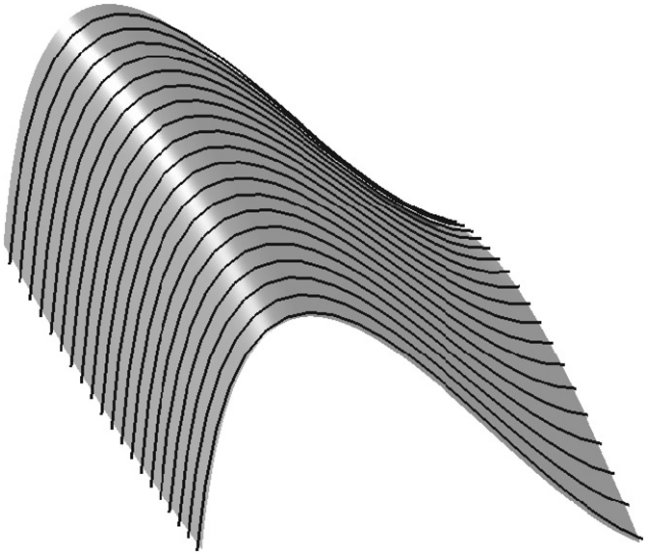

Fig. 13. CLFDM model of a Turbine blade with the FLCs in a single layer.

4. Conclusion

A new method called "Curved layer Fused Deposition Modeling" has been formulated and tested on parametric surfaces. The advantage of this method is in creating thin-section, slightly curved (shell-type) parts where the flat-layered FDM might fail to meet the strength requirements. Higher strength is obtainable by employing longer length filaments or roads and obtaining curved inter-layers of larger area per layer. The proposed method has the potential to increase strength of parts and to reduce stair-step effect, number of layers and build time simultaneously. However, capital investments would increase due to the requirement of higher sophistication in part and extruder manipulation.

Acknowledgements

We sincerely thank 'The British Journal of Oral & Maxillofacial Surgery' for granting us the permission for using Figs. 9(a) and 11. We also would like to extend our thanks to Dr. John Winder for providing the digital copies of these pictures.

References

[1] Pham DT, Dimov SS. Rapid manufacturing: The technologies and applications of rapid prototyping and rapid tooling. London: Springer-Verlag London Limited; 2001.
[2] Winder J, Bibb R. Medical rapid prototyping technologies: State of the art and current limitations for application in oral and maxillofacial surgery. Journal of Oral and Maxillofacial Surgery 2005;63:1006–15.
[3] Lee CS, Kimb SG, Kimb HJ, Ahnb SH. Measurement of anisotropic compressive strength of rapid prototyping parts. Journal of Materials Processing Technology 2007;187–188:627–30.
[4] Zhong W, Li F, Zhang Z, Song L, Li Z. Short fiber reinforced composites for fused deposition modeling. Materials Science and Engineering 2001; A301:125–30.

[5] Allen S, Dutta D. On the computation of part orientation using support structures in layered manufacturing. In: Proceedings of the fifth SFF symposium. 1994. p. 259–69.
[6] Xu F, Loh HT, Wong YS. Considerations and selection of optimal orientation for different rapid prototyping systems. Rapid Prototyping Journal 1999;5:54–60.
[7] Hu Z, Lee K, Hur J. Determination of optimal build orientation for hybrid rapid-prototyping. Journal of Materials Processing Technology 2002;130–131:378–83.
[8] Yang ZY, Chen YH, Sze WS. Layer-based machining: Recent development and support structure design. Proceedings of the Institute of Mechanical Engineers Part B: Journal of Engineering Manufacture 2002; 216(7):979–91.
[9] Dolenc A, Mäkelä I. Slicing procedures for layered manufacturing techniques. Computer-Aided Design 1994;26(2):119–26.
[10] Sabourin E, Houser SA, Bohn JH. Adaptive slicing using stepwise uniform refinement. Rapid Prototyping Journal 1996;2(4):20–6.
[11] Mani K, Kulkarni P, Dutta D. Region-based adaptive slicing. Computer-Aided Design 1999;31(5):317–33.
[12] Kulkarni P, Dutta D. An accurate slicing procedure for layered manufacturing. Computer-Aided Design 1996;28(9):683–97.
[13] Hope RL, Roth RN, Jacobs PA. Adaptive slicing with sloping layer surfaces. Rapid Prototyping Journal 1997;3(2):89–98.
[14] Ma W, But WC, He P. NURBS-based adaptive slicing for efficient rapid prototyping. Computer-Aided Design 2004;36(13):1309–25.
[15] Pandey PM, Reddy NV, Dhande SG. Real time adaptive slicing for fused deposition modelling. International Journal of Machine Tools and Manufacture 2003;43(1):61–71.
[16] Klosterman DA, Chartoff RP, Osborne NR, Graves GA, Lightman A, Han G, et al. Development of a curved layer LOM process for monolithic ceramics and ceramic matrix composites. Rapid Prototyping Journal 1999;5(2):61–71.
[17] Angle slicing of STL file for minimizing stair stepping effects. http://www.ces.clemson.edu/me/credo/projects/angslic.pdf.
[18] Kerschbaumer M, Ernst G, O'Leary P. Tool path generation for 3D laser cladding using adaptive slicing technology. In: Proceedings of the international congress on applications of lasers & electro-optics. 2005. p. 310–9.
[19] Elber G, Cohen E. Toolpath generation for freeform surface models. Computer-Aided Design 1994;26(6):490–6.
[20] Hieu LC, Zlatov N, Sloten JV, Bohez E, Khanh L, Binh PH, et al. Medical rapid prototyping applications and methods. Rapid Prototyping Journal 2005;25(4):284–92.
[21] Brown GA, Firoozbakhsh K, Decoster TA, Reyna JR, Moneim M. Rapid prototyping: The future of trauma surgery? The Journal of Bone & Joint Surgery 2003;85:49–55.
[22] Feng H-Y, Li H. Constant scallop-height tool path generation for three-axis sculptured surface machining. Computer-Aided Design 2002; 34:647–54.
[23] Ahn S-H, Montero M, Odell D, Roundy S, Wright PK. Anisotropic material properties of fused deposition modeling ABS. Rapid Prototyping Journal 2002;8(4):248–57.
[24] Bellini A, Güçeri S. Mechanical characterization of parts fabricated using fused deposition modeling. Rapid Prototyping Journal 2003;9(4):252–64.
[25] Ravi Kumar GVV, Shastry KG, Prakash BG. Computing constant offsets of a NURBS B-Rep. Computer-Aided Design 2003;35(10):935–44.
[26] Ravi Kumar GVV, Shastry KG, Prakash BG. Computing offsets of trimmed NURBS surfaces. Computer-Aided Design 2003;35(5):411–20.
[27] Piegl LA, Tiller W. Computing offsets of NURBS curves and surfaces. Computer-Aided Design 1999;31:147–56.
[28] Farouki RT. Exact offset procedures for simple solids. Computer Aided Geometric Design 1985;2:257–79.
[29] Kumar GVVR, Shastry KG, Prakash BG. Computing non-self-intersecting surfaces using of NURBS surfaces. Computer-Aided Design 2002;34(3):209–28.
[30] Amati G. A multi-level filtering approach for fairing planar cubic B-spline curves. Computer Aided Geometric Design 2007;24:53–66.